Adaptive intelligent speed control of switched reluctance motors with torque ripple reduction

Majid Hajatipour[†], Mohammad Farrokhi[†‡*]

[†]*Faculty of Electrical Engineering,*

[‡]*Center of Excellence for Power System Automation and Operation,*
Iran University of Science and Technology,
Narmak, Farjam St., Tehran 16846-13114, Iran

Abstract

Switched Reluctance (SR) motors have a wide range of applications in industries, mainly due to the special properties of this motor. But, because of its dynamical nonlinearities, its control is complex. This paper presents an adaptive intelligent control based on the Lyapunov stability theory to control the speed of SR motors with good accuracies and performances. The proposed controller composes of a speed controller and a torque controller. The main parts of the speed controller are two folds: a) the optimal controller, which is based on the Hamilton-Jacobi-Bellman theory and b) the intelligent controller, which is an adaptive fuzzy controller. The main features of the proposed speed controller are: 1) its independence to the exact parameters of the SR motor such as the inertia of rotor, the viscous friction, and the load torque, and 2) the robustness to inaccuracies and disturbances. Moreover, the torque ripple reduction is achieved by employing a neural network for torque estimation. The simulation results show good performance of the proposed controller in speed controlling and torque ripple reduction.

Keywords: Switched reluctance motor; Velocity control; Torque ripple reduction; Adaptive fuzzy control

1. Introduction

Switched reluctance (SR) motors have very interesting characteristics such as simple structure, low costs, simplicity of the power converter, and fault tolerance. Moreover, SR motors can produce high torque at low speeds. These characteristics have made the SR motors attractive for industrial applications [1-4]. Nevertheless, SR motors have highly nonlinear and dynamical behavior which makes them difficult to control. Hence, the classic linear control methods cannot provide satisfactory performances as required by the variable speed regulation and the position tracking.

In [5] and [6] the sliding-mode control has been applied for the position and speed control of SR motors. The main advantage of this kind of controller is its independence to the motor parameters, but due to employing derivative of the error in the sliding surface, it

*Corresponding author
E-mail address: farrokhi@iust.ac.ir
Tel.: (+9821) 77240492, *Fax:* (+9821) 77240490

is sensitive to the input noises and disturbances. In [7], with combination of PID and feed-forward controller, variation of speed around the operation point is reduced and consequently mechanical vibration is cancelled. But, there is a steady-state error in position. In [8] speed control of SR motors is achieved by utilizing feedback linearization method. To avoid model dependency of the controller, the authors have employed robust feedback linearization. In [9], an adaptive neuro-fuzzy controller is used as the speed and torque controller. The main duty of the fuzzy controller is to provide a compensated current signal for each phase. For this reason, the fuzzy system must be trained offline. In [2], a passivity-based method is used. The drawback of this method is that the desired phase current depends on the mathematical modeling of the motor and hence, there is need for numerical solutions. In addition, calculation of the desired torque needs numerical values for the inertia constant and the load torque. Moreover, the closed-loop stability in presence of the parameters errors has not been considered.

The proposed controller in this paper consists of two parts: the speed controller and the torque controller. The speed controller is an intelligent optimal controller, based on the Lyapunov stability theory. The speed controller itself has two main parts: 1) an adaptive intelligent controller, which is a fuzzy system that cancels out the effects of uncertainties and unknown parameters such as errors in the moment of inertia, viscous friction, and load torque and 2) an optimal controller, which forces the output to track the target. In other words, by utilizing a fuzzy system, the effects of unknown parameters in dynamical equation of the mechanical system are rejected and the model is simplified to a linear equation with known parameters. Then, an optimal control strategy is used. The output of the speed controller is the torque reference signal, which is the input to the torque controller. In the torque controller, reference signal will be compared to the estimation of the motor torque for torque ripple reduction. For this reason, a Neural Network (NN) is used to estimate the motor torque. The NN is trained with the data obtained from the Finite Element Method (FEM) when the motor is operating in the linear as well as in the saturation regions. Hence, the saturation effects in the iron core of the motor are considered.

The main advantages of the proposed method are: 1) its independence to the exact parameters of the SR motor such as the moment of inertia of rotor and viscous friction coefficients, 2) good performance in presence of the uncertainties, measurement noises, and disturbances, 3) smooth torque reference signal provided by the speed controller, and 4) torque ripple reduction by using neural networks. In addition, this controller is independent of the load torque. Performance evaluation of the proposed controller is shown through simulations using a nonlinear model of the SR motor, in which the saturation effects in the iron core are considered. Moreover, the applied voltage to the motor phases is of PWM (Pulse Width Modulation) type signal, which is common in industrial applications. Simulation results show good performance of the proposed controller.

This paper is organized as follows: First, in Section 2, a brief introduction of the SR motor will be given. Section 3 represents the proposed speed control method. The design of the torque controller will be presented in Section 4. Section 5 demonstrates the simulation results. Finally, conclusion and future works are given in Section 6.

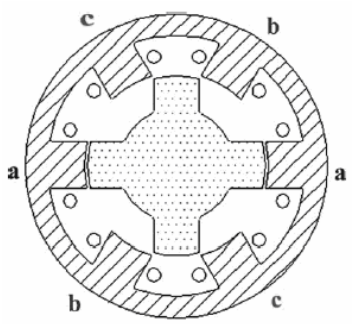

Fig. 1. Structure of a 6/4 SR motor.

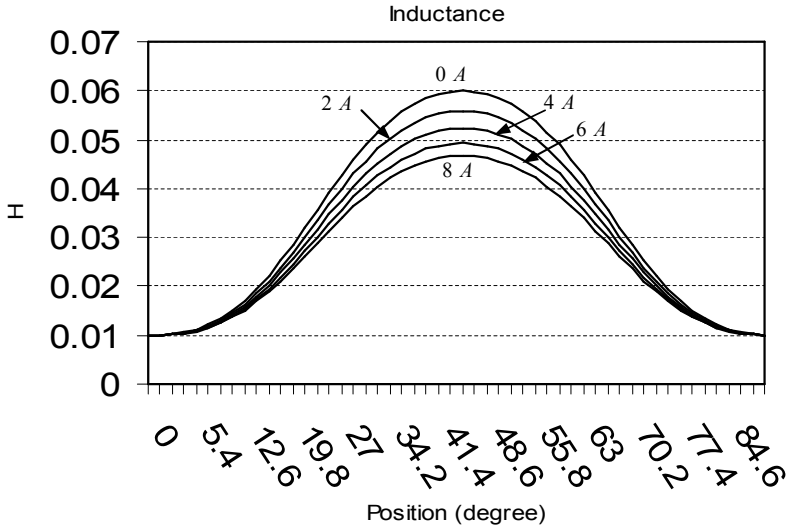

Fig. 2. Phase inductance variations with respect to the rotor position for different values of the phase current.

2. The SR motor

Fig. 1 shows the structure of a typical SR motor. This is a salient pole synchronous machine with no windings or permanent magnet on the rotor. The relationship between the voltage (V_k), the current (i_k) and the flux linkage (ψ_k) for the *k*th phase of motor is [10]

$$V_k = R\, I_k + \frac{d\psi_k}{dt}, \quad k = 1, 2, \ldots, m. \tag{1}$$

And the instantaneous generated torque is defined as

$$T_k = \frac{\partial}{\partial\theta}\int_0^i \lambda_k(\theta, i_k)\, di, \tag{2}$$

where $\lambda_k(\theta, i_k)$ is the linkage flux of the stator phase and θ is the position of rotor. Neglecting the saturation effects in the iron core, the torque produced by the *k*th phase can be simplified as

$$T_k = \frac{1}{2} i_k^2 \frac{\partial L_k(\theta)}{\partial\theta}, \tag{3}$$

where $L_k(\theta)$ is the *k*th phase inductance. Fig. 2 shows variations of the phase inductance

with respect to the position of rotor and variations in the phase current. As this Fig. shows, the phase inductance decreases when the phase current is increased. This is the indication of saturation effects in the iron core. The saturation effect is a nonlinear behavior and makes it difficult to control the speed of motor.

The relationship between the mechanical and the electrical parts of the SR motor can be written as [10]

$$J\ddot{\theta} = \sum_{k=1}^{m} T_k(\theta, I_k) - T_l - \beta\dot{\theta} \tag{4}$$

where T_l is the load torque, $T_k(\theta, I_k)$ is the generated phase torque, $\dot{\theta}$ is the angular velocity of rotor, J is the moment of inertia, β is the viscous friction coefficient, and m is the number of phases in stator.

3. Speed Control Strategy

In this section, the proposed strategy for speed control of the SR motor is described. Fig. 3 shows the block diagram of the proposed controller. The main goal of this controller is to provide the appropriate control signal (i.e. the reference torque) to the torque controller, based on the difference between the desired speed and the actual speed of the motor. In the speed control part, the task of the fuzzy system is to adaptively reject the unknown and uncertain parameters in the SR motor and in the load torque. By using this adaptive fuzzy system, the mechanical dynamics of the SR motor become linear and known. Subsequently, after simplifying the SR motor model, the Hamilton-Jacobi-Bellman theory (an optimal control method) is employed to force the tracking error to go to zero.

The position error of the motor is defined as $e_\theta = \theta_m(t) - \theta(t)$, where $\theta_m(t)$ is the reference position signal. A new variable is defined as [11]

$$r(t) = \dot{e}_\theta(t) + k_p e_\theta + k_i \int e_\theta dt \tag{5}$$

Then, using $\dot{e}_\theta = \dot{\theta}_m(t) - \dot{\theta}(t)$ and (5), it gives

$$\dot{\theta}(t) = -r(t) + \ddot{\theta}_m(t) + k_p e_\theta + k_i \int e_\theta dt \tag{6}$$

Therefore,

$$\ddot{\theta}(t) = -\dot{r}(t) + \ddot{\theta}_m(t) + k_p \dot{e}_\theta + k_i e_\theta . \tag{7}$$

It should be mentioned that in the design procedure for the speed controller, the total torque produced by each phase, which is shown as $\sum_{k=1}^{m} T_k(\theta, I_k)$ in (4), must be determined by the speed controller. This signal acts as the control signal for the speed controller. From now on, for simplicity, T_{total} will be shown by T. Substituting (7) and (6) into (4) yields

$$\dot{r}(t) = \frac{1}{J}\left[-T - \beta r(t)\right] + \left[\frac{1}{J}\left(T_l + \beta\dot{\theta}_m + \beta k_p e_\theta + \beta k_i \int e_\theta dt\right) + \left(\ddot{\theta}_m(t) + k_p \dot{e}_\theta + k_i \int e_\theta dt\right)\right], \tag{8}$$

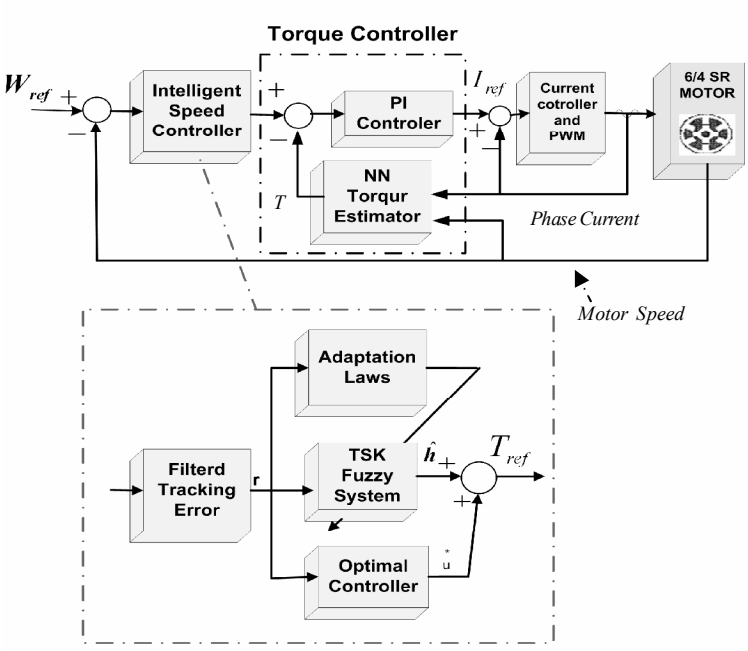

Fig. 3. Block diagram of the proposed speed and torque controllers.

where $T = \sum_{k=1}^{m} T_k\left(\theta, I_k\right)$ is the total produced torque. Here, J and β can be an approximation of their actual values. Therefore, an approximation error term should be added inside the second bracket of (8). Let define

$$h\left(\mathbf{x}, \boldsymbol{\upsilon}\right) = \left(T_l + \beta\dot{\theta}_m + \beta k_p e_\theta + \beta k_i \int e_\theta dt\right) + J\left(\ddot{\theta}_m\left(t\right) + k_p \dot{e}_\theta + k_i \int e_\theta dt\right). \tag{9}$$

Hence, (8) reduces to

$$\dot{r}\left(t\right) = \frac{1}{J}\left[-T - \beta r\left(t\right)\right] + \frac{1}{J} h\left(\mathbf{x}, \boldsymbol{\upsilon}\right), \tag{10}$$

where $\mathbf{x} = \left[\int e_\theta dt \quad e_\theta \quad \dot{e}_\theta \quad \ddot{e}_\theta\right]^T$ is the state vector and $\boldsymbol{\upsilon}$ is the vector of uncertainties and unknown parameters. Control signal of the speed controller (i.e. the total reference torque) is selected such that

$$T = h\left(\mathbf{x}, \boldsymbol{\upsilon}\right) + u, \tag{11}$$

Here, the adaptive fuzzy system is designed to approximate $h\left(\mathbf{x}, \boldsymbol{\upsilon}\right)$, and the signal u will be determined by the optimal control method. Then, using (10) and (11), the model can be simplified as

$$J\,\dot{r}\left(t\right) = -u - \beta r\left(t\right). \tag{12}$$

It shows that if the torque signal is generated as in (11), then the SR motor model will be simple and linearized. In other words, if the fuzzy system provides the exact solution to the unknown function $h\left(\mathbf{x}, \boldsymbol{\upsilon}\right)$, then the SR motor model with all uncertainties is linearized and simplified as in (12), and can be easily controlled by the optimal control methods.

Next, using (5) and (12), and defining a new state-space variable $\tilde{\mathbf{Z}}(t) = \left[\int e_\theta\, dt \quad e_\theta \quad r(t)\right]^T$, the state-space equations can be written as

$$\begin{bmatrix} e_\theta \\ \dot{e}_\theta \\ \dot{r}(t) \end{bmatrix} = \begin{bmatrix} 0 & 1 & 0 \\ -k_i & -k_p & 1 \\ 0 & 0 & -\beta/J \end{bmatrix} \begin{bmatrix} \int e_\theta\, dt \\ e_\theta \\ r(t) \end{bmatrix} + \begin{bmatrix} 0 \\ 0 \\ -1/J \end{bmatrix} u, \tag{13}$$

or in vector-matrix notation form as

$$\dot{\tilde{\mathbf{Z}}}(t) = \mathbf{A}_u \tilde{\mathbf{Z}}(t) + \mathbf{B}_u u(t). \tag{14}$$

It is important to define constants k_i and k_p such that $\mathbf{A}_u$ is a stable matrix (i.e. all its eigenvalues have negative real part).

Hence, if $h(\mathbf{x}, \mathbf{v})$ is exactly provided by the adaptive fuzzy system, then the unknown and nonlinear model of SR motor can be simplified as in (13), which is linear with known parameters. Then, the optimal control method can be used for tracking with zero error. In the next subsections, details of the adaptive fuzzy and optimal controllers are given.

3.1. Optimal Controller Design

Using the defined dynamics in (13) and using the Hamilton-Jacobi-Bellman method [12], the optimal input *u*(*t*) can be obtained such that the following cost function is minimized:

$$I = \int_0^{t_f} \left[\frac{1}{2} \tilde{\mathbf{Z}}^T(t) \mathbf{Q} \tilde{\mathbf{Z}}(t) + \frac{1}{2} u^T(t) R u(t) \right], \tag{15}$$

where $\mathbf{Q} \in \Re^{3\times 3}$ is a positive definite matrix and R is a positive constant. Then, the optimal cost function is chosen as [12]

$$I^*\left(\tilde{\mathbf{Z}}(t), t\right) = \frac{1}{2} \tilde{\mathbf{Z}}^T(t) \mathbf{K}(t) \tilde{\mathbf{Z}}(t), \tag{16}$$

where $\mathbf{K}(t)$ is

$$\mathbf{K}(t) = \begin{bmatrix} k_1 & 0 & 0 \\ 0 & k_2 & 0 \\ 0 & 0 & k_3 \end{bmatrix}.$$

Then, the optimal control input $u^*(t)$ is

$$u^*(t) = -R^{-1} \mathbf{B}_u^T \mathbf{K}(t) \tilde{\mathbf{Z}}(t). \tag{17}$$

The matrix $\mathbf{K}(t)$ is the solution of the following Riccati equation:

$$\mathbf{A}^T \mathbf{K} + \mathbf{K}\mathbf{A} + \dot{\mathbf{K}} + \mathbf{Q} - \mathbf{K}\mathbf{B}_u R^{-1} \mathbf{B}_u^T \mathbf{K} = 0. \tag{18}$$

Up to this point, it was assumed that the fuzzy system could exactly model the unknown function $h(\mathbf{x}, \mathbf{v})$. But as it is well known, fuzzy systems can only give an approximation to unknown functions; therefore, there exists approximation errors. This issue will be addressed in the next section, where the design of fuzzy system is given.

3.2.Intelligent Controller Design

The TSK[1] fuzzy system block, shown in Fig. 3, is a zero-order Sugeno fuzzy system. It consists of a set of fuzzy IF–THEN rules in the following form [13]:

$$\text{Rule}^i: \text{ IF } x_1 \text{ is } A_1^i \text{ and } \cdots \text{ and } x_n \text{ is } A_n^i, \text{ THEN } \hat{h} = \sigma_i, \tag{19}$$

where $A_1^i, \ldots, A_n^i$ are fuzzy sets and σ_i is a singleton number for the ith rule. By using the product inference engine, the centre-average defuzzifier and the singleton fuzzifier, the output of the fuzzy system can be expressed as [13]

$$\hat{h}(\mathbf{x}) = \frac{\sum_{i=1}^{p} \sigma_i \left[\prod_{j=1}^{n} \mu_{A_j^i}(x_j) \right]}{\sum_{i=1}^{p} \left[\prod_{j=1}^{n} \mu_{A_j^i}(x_j) \right]}, \tag{20}$$

where x_i $(i = 1, \ldots, n)$ are inputs to the fuzzy system, $\hat{h}(\mathbf{x})$ is the output of fuzzy system, $\mu_{A_j^i}(x_j)$ $(i = 1, 2, \ldots, p,\ j = 1, 2, \ldots, n)$ are the membership functions for fuzzy sets A_j^i, respectively, and p is the number of fuzzy rules. Equation (20) can be written in vector notation form as $\hat{h}(\mathbf{x}) = \boldsymbol{\sigma}^T \boldsymbol{\xi}(\mathbf{x})$, where $\boldsymbol{\sigma}^{\mathrm{T}} = \left[\sigma_1 \cdots \sigma_p \right]^T$ is a vector containing the adjustable parameters (i.e. the parameters in the consequent part of the fuzzy rules, given in (19)), and $\boldsymbol{\xi} = \left[\xi_1 \quad \cdots \quad \xi_p \right]^T$, in which ξ_k $(k = 1, 2, \ldots, p)$ are equal to

$$\xi_k = \frac{\prod_{j=1}^{n} \mu_{A_j^i}(x_j)}{\sum_{i=1}^{p} \left[\prod_{j=1}^{n} \mu_{A_j^i}(x_j) \right]}. \tag{21}$$

In this paper, inputs to the fuzzy system are $r(t)$ and e_θ. The role of this fuzzy system is to approximate $h(\mathbf{x}, \boldsymbol{\upsilon})$, which was defined in (9). In other word, the fuzzy system is expected to give a good estimation of the unknown parameters and uncertainties in the model of the SR motor. Hence, considering some approximation errors for the fuzzy system, it yields [14]

$$h(\mathbf{x}, \boldsymbol{\upsilon}) = \boldsymbol{\sigma}^T \boldsymbol{\xi}(\mathbf{x}) + \varepsilon(\mathbf{x}), \tag{22}$$

where $\varepsilon(\mathbf{x})$ is the approximation error. It is assumed, in this paper, that this error is bounded. I.e. $\left\| \varepsilon(\mathbf{x}) \right\| \le \varepsilon_M$, where ε_M is a positive number. Therefore, the output of the fuzzy system can be written as

$$\hat{h}(\mathbf{x}, \boldsymbol{\upsilon}) = \hat{\boldsymbol{\sigma}}^T \boldsymbol{\xi}(\mathbf{x}). \tag{23}$$

For disturbance rejection, a robust term u_s can be added to the control signal [15]. Hence, the control signal of the speed controller becomes

[1] Takagi-Sugeno-Kang

$$T = \hat{\boldsymbol{\sigma}}^T \boldsymbol{\xi}(\mathbf{x}) + u^* + u_s, \tag{24}$$

where the robust term u_s can be calculated as [16]

$$u_s = \kappa_z \frac{r(t)}{|r(t)|} = \kappa_z \operatorname{sgn}(r(t)), \tag{25}$$

in which $\operatorname{sgn}(r(t)) = 1$ if $r(t) > 0$, $\operatorname{sgn}(r(t)) = -1$ if $r(t) < 0$, and κ_z is a positive constant. In order to reduce the chattering effects, $\operatorname{sgn}(r(t))$ can be replaced by $\operatorname{sat}(r(t))$ [16].

Next, the effect of model disturbances is considered. Substituting (22), (23), and (24) into (10), and denoting the external disturbances with τ_d, it gives

$$J\dot{r}(t) = \tilde{\boldsymbol{\sigma}}^T \boldsymbol{\xi}(\mathbf{x}) - u^* - \beta r(t) + \varepsilon(\mathbf{x}) + \tau_d - u_s, \tag{26}$$

where $\tilde{\boldsymbol{\sigma}} = \boldsymbol{\sigma}^* - \hat{\boldsymbol{\sigma}}$, in which $\boldsymbol{\sigma}^*$ is the optimal value of $\boldsymbol{\sigma}$, and $\varepsilon(\mathbf{x})$ is the approximation error of the fuzzy system, which is assumed to be bounded. Therefore, using (13), (14) and (26), the state-space equation can be rewritten as

$$\dot{\tilde{\mathbf{Z}}} = \mathbf{A}_u \tilde{\mathbf{Z}} + \mathbf{B}_u \left[u^* - \tilde{\boldsymbol{\sigma}}^T \boldsymbol{\xi}(\mathbf{x}) - \varepsilon(\mathbf{x}) - \tau_d + u_s \right]. \tag{27}$$

Hence, the main goal in the speed controller is to develop an algorithm to find $\hat{\boldsymbol{\sigma}}$ and u_s such that $\tilde{\boldsymbol{\sigma}}$ and $\tilde{\mathbf{Z}}$ (i.e. both the estimation error and the tracking error) remain bounded and as small as possible. To achieve this, an algorithm, based on the Lyapunov stability theory, will be proposed in the next section.

3.3.The Adaptation Law

In this section, the adaptation law for the fuzzy variable $\hat{\boldsymbol{\sigma}}$ is introduced such that the closed-loop stability is guaranteed. But, first, some definitions are in order.

Definition: Given matrixes $\mathbf{A}$ and $\mathbf{B}$, the Frobenius norm is defined as $\|\mathbf{A}\|_F = \operatorname{tr}(\mathbf{A}^T \mathbf{A})$ with $\operatorname{tr}(\cdot)$ as the trace operator. The associated inner product is $\langle \mathbf{A}, \mathbf{B} \rangle_F = \operatorname{tr}(\mathbf{A}^T \mathbf{B})$.

Lemma: The Frobenius norm is compatible with the two-norm such that $\|\mathbf{A}\mathbf{x}\|_2 \le \|\mathbf{A}\|_F \|\mathbf{x}\|_2$ with $\mathbf{A} \in \Re^{m \times n}$ and $\mathbf{x} \in \Re^n$ [17].

Theorem: Consider the nonlinear SR motor model presented in (4) and (10), and assume that the intelligent optimal control is as in (24). Then, the following adaptation law, for updating the parameters of the fuzzy system, guarantees the stability of the closed-loop system:

$$\dot{\hat{\boldsymbol{\sigma}}} = -\mathbf{F}\boldsymbol{\xi}(\mathbf{x})\mathbf{B}_u^T \mathbf{K}\tilde{\mathbf{Z}} - \kappa \|\tilde{\mathbf{Z}}\| \hat{\boldsymbol{\sigma}}. \tag{28}$$

where $\mathbf{F} = \mathbf{F}^T > \mathbf{0}_{n \times n}$ is a diagonal matrix and adjusts the rate of convergence for the fuzzy parameters (in the simplest case, this matrix can be an identity matrix), and $\kappa > 0$.

Proof: Let define the following Lyapunov function:

$$V = \frac{1}{2}\tilde{\mathbf{Z}}^T \mathbf{K}\tilde{\mathbf{Z}} + \frac{1}{2}\mathrm{tr}\left(\tilde{\boldsymbol{\sigma}}^T \mathbf{F}^{-1}\tilde{\boldsymbol{\sigma}}\right). \tag{29}$$

The time derivative of V becomes

$$\dot{V} = \tilde{\mathbf{Z}}^T \mathbf{K}\dot{\tilde{\mathbf{Z}}} + \frac{1}{2}\tilde{\mathbf{Z}}^T \dot{\mathbf{K}}\tilde{\mathbf{Z}} + \mathrm{tr}\left(\tilde{\boldsymbol{\sigma}}^T \mathbf{F}^{-1}\dot{\tilde{\boldsymbol{\sigma}}}\right). \tag{30}$$

Substituting (18) and (27) into (30) yields

$$\begin{aligned}\dot{V} = {} & \tilde{\mathbf{Z}}^T \mathbf{K}\mathbf{A}_u\tilde{\mathbf{Z}} - \tilde{\mathbf{Z}}^T \mathbf{K}\mathbf{B}_u R^{-1}\mathbf{B}_u^T \mathbf{K}\tilde{\mathbf{Z}} + \frac{1}{2}\tilde{\mathbf{Z}}^T \dot{\mathbf{K}}\tilde{\mathbf{Z}} + \mathbf{Z}^T \mathbf{K}\mathbf{B}_u\left\{-\tilde{\boldsymbol{\sigma}}^T \boldsymbol{\xi}(\mathbf{x}) - \varepsilon(\mathbf{x}) - \tau_d + u_s\right\} \\ & + \mathrm{tr}\left(\tilde{\boldsymbol{\sigma}}^T \mathbf{F}^{-1}\dot{\tilde{\boldsymbol{\sigma}}}\right).\end{aligned} \tag{31}$$

Using the Riccati equation (18) and considering that $\tilde{\mathbf{Z}}^T \mathbf{K}\mathbf{A}\tilde{\mathbf{Z}} = \frac{1}{2}\tilde{\mathbf{Z}}^T\left\{\mathbf{A}^T\mathbf{K} + \mathbf{K}\mathbf{A}\right\}\tilde{\mathbf{Z}}$, it gives

$$\frac{1}{2}\mathbf{A}^T\mathbf{K} + \frac{1}{2}\mathbf{K}\mathbf{A} + \frac{1}{2}\dot{\mathbf{K}} = -\frac{1}{2}\mathbf{Q} + \frac{1}{2}\mathbf{K}\mathbf{B}_u R^{-1}\mathbf{B}_u^T\mathbf{K}. \tag{32}$$

Therefore, the time derivative of Lyapunov function becomes

$$\dot{V} = -\frac{1}{2}\tilde{\mathbf{Z}}^T \mathbf{Q}\tilde{\mathbf{Z}} - \frac{1}{2}\tilde{\mathbf{Z}}^T \mathbf{K}\mathbf{B}_u R^{-1}\mathbf{B}_u^T \mathbf{K}\tilde{\mathbf{Z}} + \mathbf{Z}^T \mathbf{K}\mathbf{B}_u\left\{-\varepsilon(\mathbf{x}) - \tau_d + u_s\right\} + \mathrm{tr}\left(\tilde{\boldsymbol{\sigma}}^T\left(\mathbf{F}^{-1}\dot{\tilde{\boldsymbol{\sigma}}} - \boldsymbol{\xi}\mathbf{B}_u^T\mathbf{K}\tilde{\mathbf{Z}}\right)\right). \tag{33}$$

And then,

$$\begin{aligned}\dot{V} = {} & -\frac{1}{2}\tilde{\mathbf{Z}}^T \mathbf{Q}\tilde{\mathbf{Z}} - \frac{1}{2}\tilde{\mathbf{Z}}^T \mathbf{K}\mathbf{B}_u R^{-1}\mathbf{B}_u^T \mathbf{K}\tilde{\mathbf{Z}} + \tilde{\mathbf{Z}}^T \mathbf{K}\mathbf{B}_u\left\{-\varepsilon(\mathbf{x})\right\} + \tilde{\mathbf{Z}}^T \mathbf{K}\mathbf{B}_u\left\{-\tau_d + u_s\right\} \\ & + \mathrm{tr}\left(\tilde{\boldsymbol{\sigma}}^T\left(\mathbf{F}^{-1}\dot{\tilde{\boldsymbol{\sigma}}} - \boldsymbol{\xi}\mathbf{B}_u^T\mathbf{K}\tilde{\mathbf{Z}}\right)\right).\end{aligned} \tag{34}$$

Hence,

$$\begin{aligned}\dot{V} \le {} & -\frac{1}{2}\tilde{\mathbf{Z}}^T \mathbf{Q}\tilde{\mathbf{Z}} - \frac{1}{2}\tilde{\mathbf{Z}}^T \mathbf{K}\mathbf{B}_u R^{-1}\mathbf{B}_u^T \mathbf{K}\tilde{\mathbf{Z}} + \left\|\tilde{\mathbf{Z}}\right\|\varepsilon_M + \left\|\tilde{\mathbf{Z}}^T \mathbf{K}\mathbf{B}_u\right\|\left|\tau_d\right| \\ & + \tilde{\mathbf{Z}}^T \mathbf{K}\mathbf{B}_u u_s + \mathrm{tr}\left(\tilde{\boldsymbol{\sigma}}^T\left(\mathbf{F}^{-1}\dot{\tilde{\boldsymbol{\sigma}}} - \boldsymbol{\xi}\mathbf{B}_u^T\mathbf{K}\tilde{\mathbf{Z}}\right)\right).\end{aligned} \tag{35}$$

where ε_M is the maximum error of fuzzy approximation. In order to guarantee the robustness of closed-loop system, κ_z in (25) can be chosen such that

$$\kappa_z \ge \left|\tau_d\right|. \tag{36}$$

Since

$$\tilde{\mathbf{Z}}^T \mathbf{K}\mathbf{B}_u = -r(t)\frac{k_3}{j}$$

and

$$\frac{r(t)\frac{k_3}{J}}{\left|r(t)\frac{k_3}{J}\right|} = \mathrm{sgn}\left(r(t)\right)$$

then, by substituting (25) into (35) and considering (36), it yields

$$\dot{V} \le -\frac{1}{2}\tilde{\mathbf{Z}}^T \mathbf{Q}\tilde{\mathbf{Z}} - \frac{1}{2}\tilde{\mathbf{Z}}^T \mathbf{K}\mathbf{B}_u R^{-1}\mathbf{B}_u^T \mathbf{K}\tilde{\mathbf{Z}} + \left\|\tilde{\mathbf{Z}}\right\|\varepsilon_M + \mathrm{tr}\left(\tilde{\boldsymbol{\sigma}}^T\left(\mathbf{F}^{-1}\dot{\tilde{\boldsymbol{\sigma}}} - \boldsymbol{\xi}\mathbf{B}_u^T \mathbf{K}\tilde{\mathbf{Z}}\right)\right). \tag{37}$$

Now, consider the following inequality:

$$\mathrm{tr}\left(\tilde{\boldsymbol{\sigma}}^T\left(\boldsymbol{\sigma} - \tilde{\boldsymbol{\sigma}}\right)\right) = \left\langle \tilde{\boldsymbol{\sigma}}, \boldsymbol{\sigma}\right\rangle - \left\|\tilde{\boldsymbol{\sigma}}\right\|_F^2 \le \left\|\tilde{\boldsymbol{\sigma}}\right\|_F \sigma_M - \left\|\tilde{\boldsymbol{\sigma}}\right\|_F^2, \tag{38}$$

where σ_M is the maximum element of vector $\boldsymbol{\sigma}$. Then, substituting (28) and (38) into (37) gives

$$\dot{V} \le -\frac{1}{2}\left\|\tilde{\mathbf{Z}}\right\|^2\left\{\lambda_{\min}\left(\mathbf{Q}\right) + R^{-1}\right\} + \left\|\tilde{\mathbf{Z}}\right\|\varepsilon_M + \kappa\left\|\tilde{\mathbf{Z}}\right\|\left(\left\|\tilde{\boldsymbol{\sigma}}\right\|_F \sigma_M - \left\|\tilde{\boldsymbol{\sigma}}\right\|_F^2\right). \tag{39}$$

Rearranging (39) yields

$$\dot{V} \le -\frac{1}{2}\left\|\tilde{\mathbf{Z}}\right\|\left[\left\|\tilde{\mathbf{Z}}\right\|\left\{\lambda_{\min}\left(\mathbf{Q}\right) + R^{-1}\right\} + \kappa\left(\left\|\tilde{\boldsymbol{\sigma}}\right\|_F - \frac{1}{2}\sigma_M\right)^2 - \varepsilon_M - \frac{1}{4}\kappa\sigma_M^2\right]. \tag{40}$$

In order to guarantee $\dot{V} \le 0$, terms inside the bracket of (40) must remain positive. Therefore, the convergence of parameters and the stability condition can be defined as the following inequalities:

$$\left\|\tilde{\mathbf{Z}}\right\| \ge \frac{\varepsilon_M + \frac{1}{4}\kappa\sigma_M^2}{\lambda_{\min}\left(\mathbf{Q}\right) + R^{-1}} \triangleq B_{\tilde{Z}}, \tag{41}$$

$$\left\|\tilde{\boldsymbol{\sigma}}\right\|_F \ge \sqrt{\varepsilon_M + \frac{1}{4}\kappa\sigma_M^2} + \frac{1}{2}\sigma_M \triangleq B_{\hat{\sigma}}, \tag{42}$$

where $B_{\hat{\sigma}}$ and $B_{\tilde{Z}}$ can be considered as the convergence regions. □

Remark 1: According to (41) and (42), if the filtered error $r(t)$ and the approximation error in the fuzzy system $\tilde{\boldsymbol{\sigma}}(t)$ exceed a certain but bounded value, then the closed-loop system becomes stable; because the derivative of Lyapunov function becomes negative, which forces the system to go back to the stable region.

Remark 2: The proof of the above theorem shows that the variables $e_\theta(t)$, $r(t)$, and $\tilde{\boldsymbol{\sigma}}(t)$ are bounded at all time.

Remark 3: The convergence regions $B_{\hat{\sigma}}$ and $B_{\tilde{Z}}$ can be made small by selecting appropriate values for R^{-1} and κ.

Remark 4: Speed tracking implies torque tracking (i.e., when the speed tracking error is bounded, then the torque tracking error remains bounded as well). This is shown in the following Corollary:

Corollary: The adaptation law in (28) guarantees that the torque tracking error remains bounded.

Proof: By using (4) and (24), the difference between the generated torque and the desired torque can be written as

$$\sum_{k=1}^{m} T_k(\theta, I_k) - T_d = \left(J\ddot{\theta} + \beta\dot{\theta} + T_l\right) - \left(\hat{\boldsymbol{\sigma}}^T \boldsymbol{\xi}(\mathbf{x}) + u^* + u_s\right). \tag{43}$$

in which $\sum_{k=1}^{m} T_k(\theta, I_k)$ is the torque signal generated by the phases of SR motor (estimated by the torque estimator in the torque controller part), and T_d is output of the speed controller that acts as the reference torque for the torque controller. Then, substituting (6) and (7) into (43) and using (17) and (25), it yields

$$\begin{aligned} \sum_{k=1}^{m} T_k(\theta, I_k) - T_d &= h(\mathbf{x}, \mathbf{v}) - \hat{\boldsymbol{\sigma}}^T \boldsymbol{\xi}(\mathbf{x}) - \left(u^* + u_s\right) \\ &= \boldsymbol{\sigma}^T \boldsymbol{\xi}(\mathbf{x}) + \varepsilon(\mathbf{x}) - \hat{\boldsymbol{\sigma}}^T \boldsymbol{\xi}(\mathbf{x}) - \frac{k_3}{J} R^{-1} r(t) - \kappa_z \operatorname{sat}\left(r(t)\right) \\ &= \tilde{\boldsymbol{\sigma}}^T \boldsymbol{\xi}(\mathbf{x}) + \varepsilon(\mathbf{x}) - \frac{k_3}{J} R^{-1} r(t) - \kappa_z \operatorname{sat}\left(r(t)\right). \end{aligned} \tag{44}$$

According to the above theorem, $\tilde{\boldsymbol{\sigma}}$ and $r(t)$ are bounded and can be made small; moreover $\left\|\varepsilon(\mathbf{x})\right\| \le \varepsilon_M$. Then, according to (44), it is clear that torque-tracking error remains bounded too. □

Hence, the proved theorem, which guarantees stability of the speed controller, indirectly guarantees stability of the torque controller as well. Notice that, this argument is correct only if $\sum_{k=1}^{m} T_k(\theta, I_k)$ in (4) (i.e. the torque generated by the phases of the SR motor) is estimated with good accuracy in the torque controller part. In this paper, $\sum_{k=1}^{m} T_k(\theta, I_k)$ is estimated using a neural network. This network is trained off-line using experimental data. This issue will be addressed in the next section.

4. Torque Controller Design

Generally, there are two approaches for torque control in SR motors. The first approach, which is used commonly, is based on neglecting the saturation effects in the iron core. In this situation, relationship between the produced torque and current of the stator phase is linear and can be written as [2]

$$T_n = \frac{\partial W_c}{\partial \theta} = \frac{\partial \left\{ \int_0^i \left[L_n(i_n, \theta) i_n \right] di \right\}}{\partial \theta} = \frac{1}{2} i_n^2 \frac{\partial L_n(\theta)}{\partial \theta}, \tag{45}$$

where W_c is the co-energy. From (45), the relationship between the reference torque and the reference current in the stator phase can be easily derived as

$$i_{\text{ref}} = \left[\frac{2T_{\text{d}}}{\partial L(\theta) / \partial \theta} \right]^{1/2} . \tag{46}$$

But the main drawback of this approach is that it does not consider the saturation effects in the iron core. In the saturation region, the relationship between the phase current and the torque becomes nonlinear. Consequently, the torque ripple becomes considerably large, which increases the mechanical vibration of motor.

One of the main reasons for torque ripple generation in SR motors is neglecting the nonlinear relationship between the phases current and the produced torque, and the position of rotor.

In the second approach, a torque estimator is used. In this paper, a neural network is employed to estimate the generated torque of the SR motor. This network is trained off-line using data acquired form both the linear region and the saturation region. It will be shown, in simulations, that the second approach is very effective in torque ripple reduction. Moreover, it is more realistic, since it considers the saturation effects in the iron core.

4-1 Proposed Torque Controller

In view of (2) and considering that the phase inductance is a function of the phase current and position of the rotor (i.e. taking the saturation effects of the iron core into account), the relationship between the phase current and the phase torque becomes nonlinear. Based on this, a controller is designed in this section that consists of two parts: 1) a neural network, which estimates the total generated phases torque based on the phase current and the rotor position, and 2) a PI controller, which provides the phase reference current (Fig. 3).

In this approach, the error between the reference torque, which is provided by the speed controller, and the estimated torque, which is given by the neural network, is the input to a PI controller. The output of the PI controller is the reference current. For the neural network part, a Multilayer Perceptron (MLP) is employed. The general structure of an MLP is shown in Fig. 4. Adjustable parameters are the synaptic weights connecting neurons of layers [15]. Inputs to the MLP are the phase current and the position of rotor. The output of the network is the estimated phase torque. The training data for the neural network is acquired form one period operation of the SR motor (i.e. from unaligned position to the aligned position of rotor). Hence, the saturation effect of the iron core is considered in the motor model. Therefore, the neural network takes the phase current and the rotor position as inputs, and estimates the desired torque based on (2). In the training procedure, the phase current is in the range of [0, $I_{\max}$] whereas this range for the position of rotor is [$0^{\circ}, 50^{\circ}$] (0° for the unaligned position and 45° for the aligned position). One of the most common methods for training an MLP is the error back-propagation algorithm, in which weights are adjusted to minimize a predefined cost function as [18]

$$\mathrm{E} = \frac{1}{2} \sum_{i=1}^{l} e_i^2 \tag{45}$$

$$\mathbf{w}(n+1) = \mathbf{w}(n) - \eta \frac{\partial \mathrm{E}(n)}{\partial \mathbf{w}(n)} \tag{46}$$

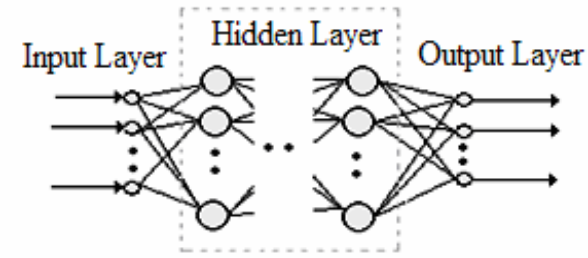

Fig. 4. Structure of an MLP neural network.

where $\mathbf{w}(n)$ is a vector containing all the adjustable weights of the neural network, $\frac{\partial \mathrm{E}(n)}{\partial \mathbf{w}(n)}$ is the gradient of error function with respect to weights, and η is the learning rate [18].

5. Simulations

In this section, the proposed controller is implemented to control the nonlinear model of a 6/4 SR motor (6 and 4 are the number of stator and rotor poles, respectively). Motor specifications are given in Table 1. In addition, the Finite Element Method (FEM) is employed for modeling the SR motor. Using this method, the data are stored form each phase in a lookup table. As it is clear from Fig. 2, saturation effect is considered in the modeling. As it was mentioned in section 3.2, the adjustable parameter of the fuzzy system is the variable $\boldsymbol{\sigma}$ in (19). The Gaussian fuzzy membership functions for the input variables $r(t)$ and $e_\theta(t)$ are shown in Fig. 5. The initial values for vector $\boldsymbol{\sigma}$ (i.e. the center of membership functions for the THEN part of the fuzzy rules) are distributed evenly in the range of signal variations as

$$\boldsymbol{\sigma}(0)=\begin{bmatrix}-0.4 & -0.3 & -0.2 & -0.1 & 0 & 0.1 & 0.2 & 0.3 & 0.4\end{bmatrix}^T .$$

For the speed controller, some parameters, such as R^{-1}, κ and $\mathbf{F}$, must be regulated. Figs. 6-9 show performance of the proposed controller with different values for R^{-1} and κ. Matrix $\mathbf{F}$ is selected simply as an identity matrix. In the torque controller part, the best coefficients for PI controller are determined such that response of the torque control loop is fast enough; however, the proposed controller is not very sensitive to these coefficients. In the simulations $k_p = 400$ and $k_i = 40$ are selected.

The neural network has 2 inputs (the phase current and the position of rotor), 2 hidden layers, with 40 and 20 neurons in the first and the second hidden layer, respectively, and one output (the estimated phase torque). The nonlinear activation function of neurons is of tangent hyperbolic type and the learning rate is 0.1.

Simulation results show that the proposed controller is able to reduce effectively the torque ripples in the linear region as well as in the saturation region. In the following sections, the performance of the proposed controllers is evaluated.

5.1.Speed Controller Evaluation

In this part of simulation, the proposed speed controller is evaluated for different values of its parameters (Figs. 6-9). As it is clear from Figs. 6 and 7, increasing R^{-1} yields faster response for the speed signal and at the same time decreases convergence region $B_{\tilde{Z}}$, according to (41). Moreover, increasing this parameter increases torque reference signal (output of the speed controller signal) due to (15) and (17). Fig. 8 shows how the proposed controller reacts to parameter κ. Increasing κ yields more oscillations in the fuzzy signal, according to (28). This in turn, increases convergence, according to (41) (Fig. 9).
Fig. 10 shows the reference torque signal, produced by the speed controller and the generated torque signal for a sample torque load of 0.2 NM. Moreover, Fig. 11 shows the related torques and currents.

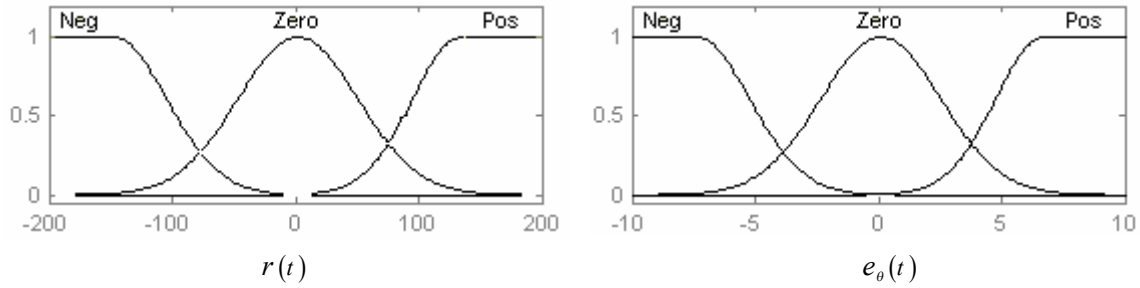

$r(t)$ $\qquad\qquad$ $e_\theta(t)$

Fig. 5. Membership functions for fuzzy system inputs $r(t)$ and $e_\theta(t)$.

Table 1
Parameters of the SR motor

Parameter	Value
Stator poles	6
Rotor poles	4
DC voltage	100 V
Stator resistance	$0.5\,\Omega$
Moment of inertia	0.0002 Nms
Viscous friction coefficient	0.00018 Nms^2
Maximum phase inductance	60 mH
Minimum phase inductance	10 mH

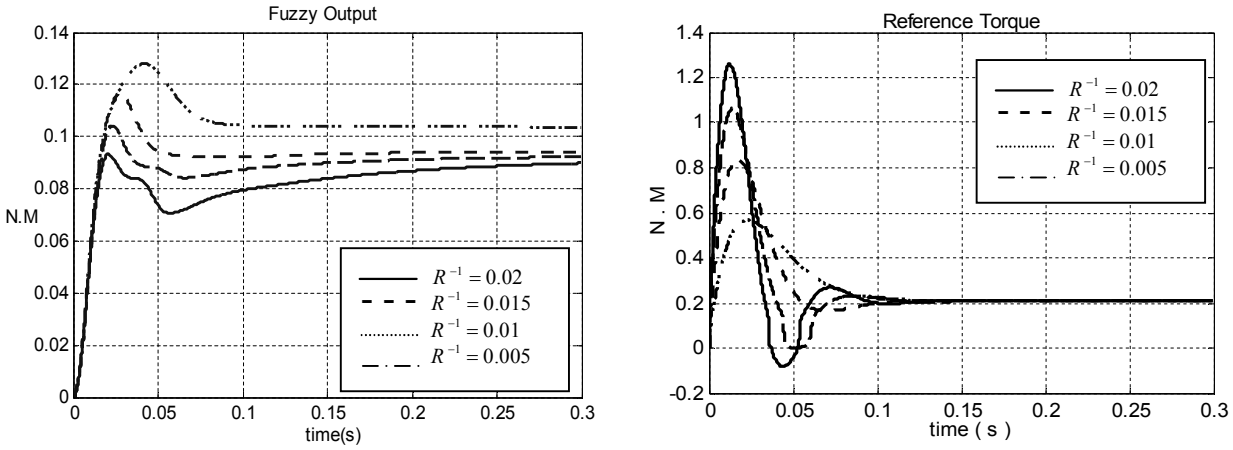

(a) $\qquad\qquad$ (b)

Fig. 6. (a) Output of the fuzzy system and (b) Reference torque, for different values of R^{-1}.

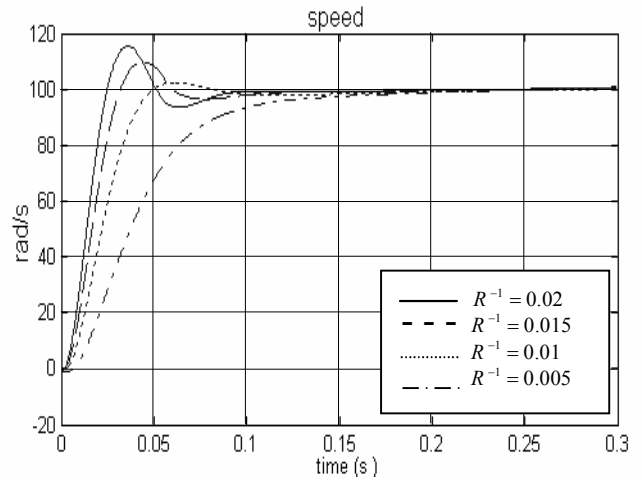

Fig. 7. Speed of the SR motor for different values of R^{-1}

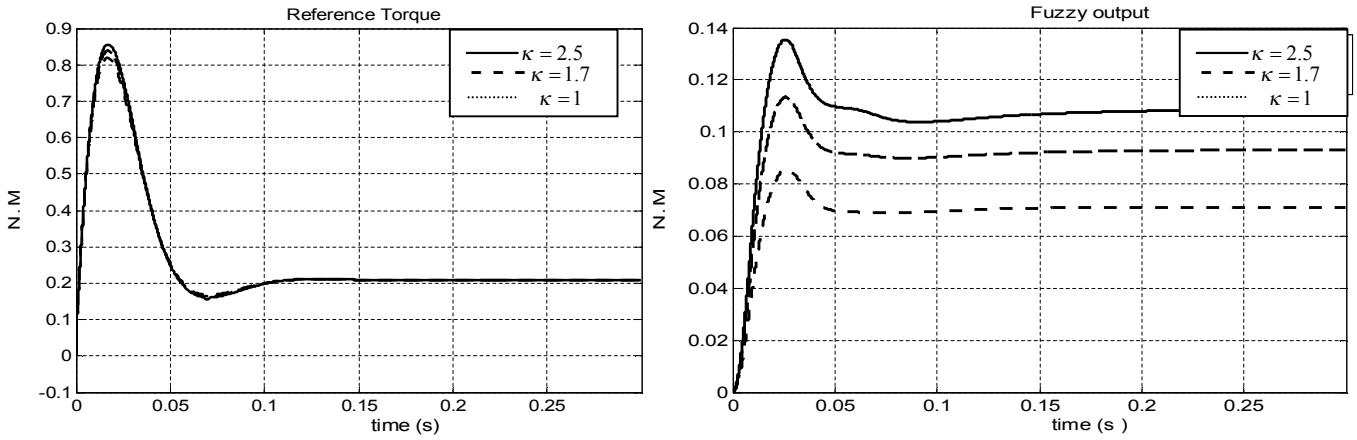

(a) (b)

Fig. 8. (a) Output of the fuzzy system and (b) Reference torque for different values of κ .

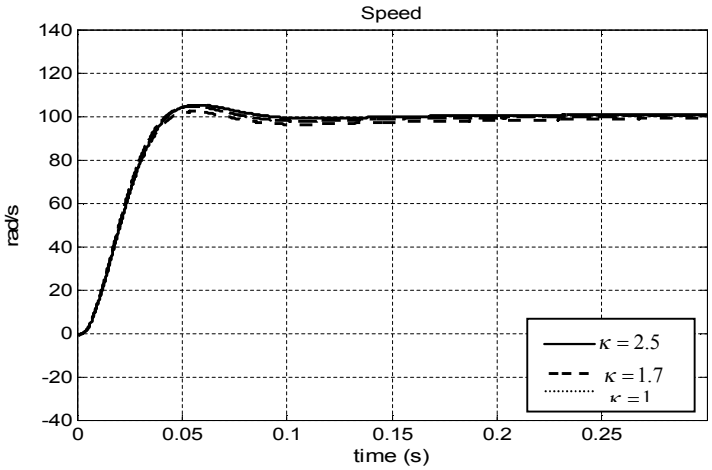

Fig. 9. Speed of the SR motor for different values of κ .

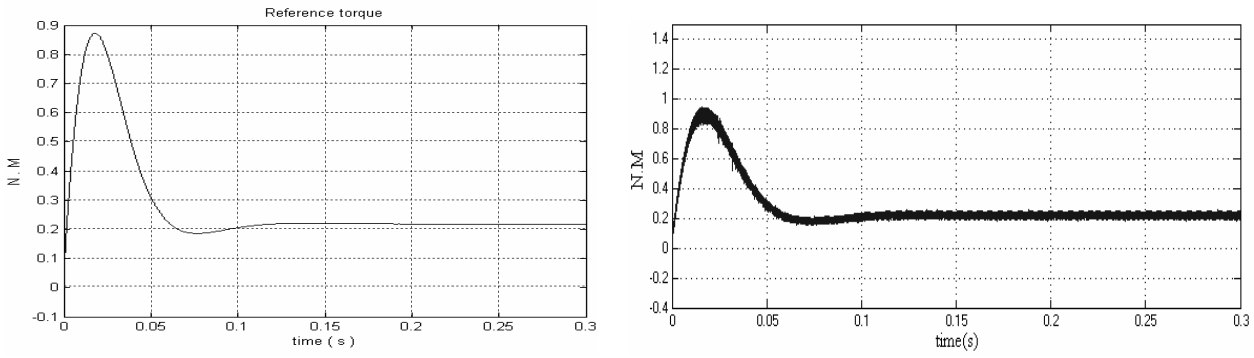

(a) (b)

Fig. 10. (a) Reference torque and (b) generated torque, of the SR motor controller for load torque = 0.2 N.M

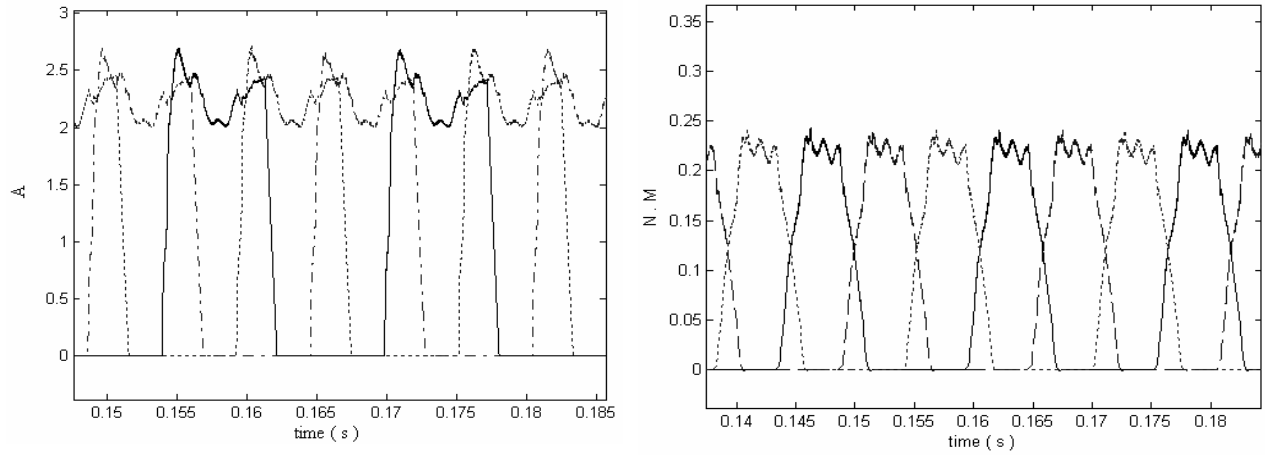

(a) (b)

Fig. 11. (a) Phase currents and (b) phase torques, for Fig. 10.

5.2. Torque Controller Evaluation

In this section, performance of the proposed torque controller is evaluated by operating in the saturation region. In this case, load torque is large enough to force the SR motor to operate in the saturation region.

By increasing the load torque to 1 N.M, the torque controller, which is based on estimation of the phase torque by the neural network, effectively reduces torque ripples (Figs. 12). Fig. 13 shows the phase currents and the phase torques in the case of load torque equal to 1 N.M. In addition to the torque ripple reduction, one of the main benefits of using the neural network to model nonlinearities of the SR motor is smooth variations of the required phases current (Fig.13). Sharp peaks in phases current can cause difficulties in practice.

5.3. Load Disturbance Rejection

In this part, performance of the proposed controller will be evaluated in presence of load disturbance. At $t = 0.3\,\mathrm{s}$, load disturbance equal to 0.1 N.M. is exerted to the rotor. Due to the use of a robustifying term u_s in the control signal, load disturbance is rejected quickly

(Fig. 14). Fig. 15 shows the generated motor torque in presence of the applied load disturbance.

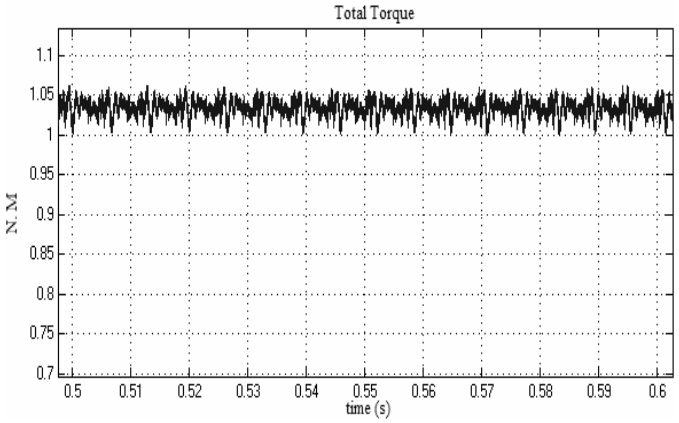

Fig. 12. Torque generated by the SR motor when load torque = 1 N.M.

(a) (b)

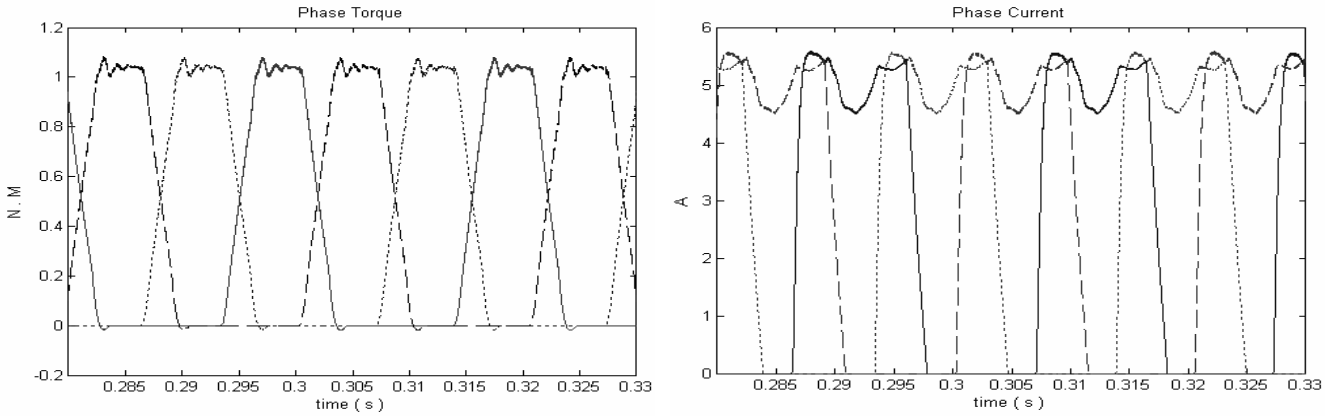

Fig. 13. (a) phase torques and (b) phase currents when load torque = 1 N.M.

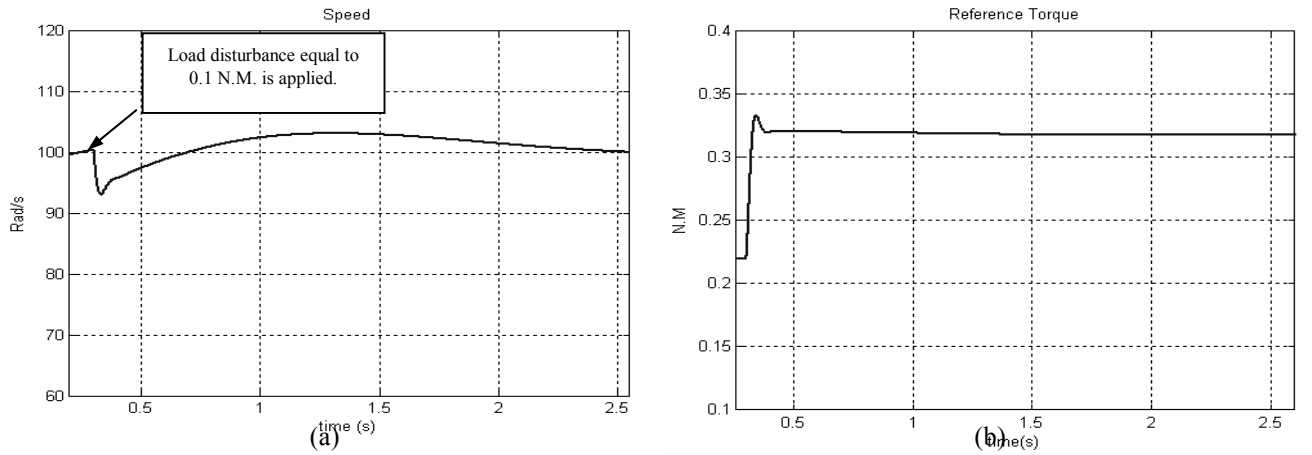

(a) (b)

Fig. 14. Performance of the proposed controller in presence of load disturbances, (a) angular speed and (b) reference torque (disturbance is applied at t = 0.3 s).

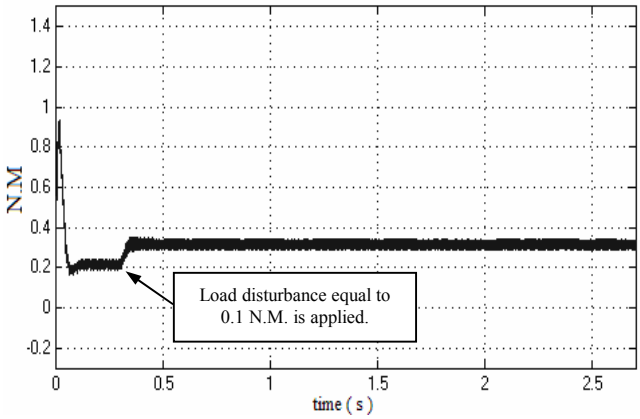

Fig. 15. Torque generated by the SR motor in presence of load disturbance (applied at $t = 0.3$ s).

6. Conclusion and Future Work

In this paper, a new adaptive method for controlling speed and torque of switched reluctance motors was introduced. This controller can effectively reject disturbances as well as uncertainties in parameters of the motor that are present in almost all practical applications. The speed controller consists of two main components: 1) an adaptive intelligent controller, which is a Sugeno-type fuzzy system and approximates the load torque, the error in moment of inertia, and the viscous friction, and 2) an optimal controller, which forces the output of the system optimally track the target signal. In addition, the stability of the speed controller was guaranteed using the Lyapunov stability theory. Moreover, torque ripple reduction was achieved by applying a neural network torque estimator, which was trained off-line using motor data, obtained from finite-element method. Inputs to the neural network were the phase current and the actual position the SR motor. The error between the reference torque and the output of the neural network is input to a PI controller, which was used as a torque controller. The simulation results showed effectiveness of the proposed controller in torque ripple reduction. In addition, the phase currents, in the proposed torque controller, have smooth variations. Future works of this research include: 1) performing analytical work on the stability of the closed-loop system when both the speed controller and the torque controller are present, 2) applying optimal control in the torque control strategy and defining the cost function, in which some important factors of the SR motor, such as radial force variations and energy consumption, is considered.

References

[1] Qionghua Z, Shuanghong W. Optimum design of switched reluctance motors using dynamic finite element analysis. IEEE Trans Magnetics 1997; 33(2): 2033-6.

[2] Perez GE, Ortiz PM. Passivity-based control of switched reluctance motors with nonlinear magnetic circuits. IEEE Trans Control System Technology 2004; 12(3): 439-48.

[3] McCann R, Islam M. Application of a sliding-mode observer for position and speed estimation in switched reluctance motor drives. IEEE Trans Ind Appl 2001; 37(1): 51-8.

[4] Yamai H, Kaneda M. Optimal switched reluctance motor drive for hydraulic pump unit. Proc IEEE Int Conf Ind Appl, Italy, Rome 2000: 1555-62.

[5] Reay DS, Mirkazemi M. On the appropriate uses of fuzzy systems: fuzzy sliding mode position control of a switched reluctance machine. Proc IEEE Conf Ind Appl, Monterey 1995: 371-6.
[6] Forrai A, Biro Z. Sliding mode control of switched reluctance motor. Proc IEEE Int Conf Optimization of Electrical and Electronic Equipments, Romania 1998: 467-72.
[7] Hussain SA, Hussain I. Outer Loop Controller Design of a Switched Reluctance Motor Driven System. Proc IEEE Int Conf Ind Appl, Salt Lake City, Utah 2003: 486-91.
[8] Panda SK, Dash PK. Application of nonlinear control to switched reluctance Motors: a Feedback Linearization Approach. IEE Proc.-Electr**.** Power Appl 1996: 143(5).
[9] Akcayol MA. Application of adaptive neuro-fuzzy controller for SRM. Elsevier Journal on Advances in Engineering Software 2004: 129-37.
[10] Henriques LO, Branco PJ. Proposition of an Offline Learning Current Modulation for Torque-Ripple Reduction in Switched Reluctance Motors: Design and Experimental Evaluation. IEEE Trans Ind Electronics 2002, 49(3): 665-76.
[11] Wai RJ, Lee MC. Intelligent Optimal Control of Single-Link Flexible Robot Arm. IEEE Trans Industrial Electronics 2004; 51(1): 201-20.
[12] Kirk DE. Optimal Control Theory. New Jercy: Prentice-Hall; 1970.
[13] Wang LX. A Course in Fuzzy Systems and Control. New Jercy: Prentice Hall; 1997.
[14] Kim YH, Lewis FL. Optimal Design of CMAC Neural-Network Controller for Robot Manipulators. IEEE Trans Sys Man and Cybern. 2000; 30(1): 22- 30.
[15] El-Hawwary MI, Elshafei AL, Output feedback control of a class of nonlinear systems using direct adaptive fuzzy controller. IEE Proc.-Control Theory Appl. 2004, 151(5): 615-624
[16] Slotine JJ. Applied Nonlinear Control. , New Jersey: Prentice Hall; 1991.
[17] Horn RA, Johnson CR, Matrix Analysis, Cambridge University Press; 1985.
[18] Haykin S. Neural Networks, A Comprehensive Foundation. New Jersey: Prentice Hall; 1999.